

# Precise Density Measurement of Liquid Titanium by Electrostatic Levitator

Shumpei Ozawa<sup>1,\*1</sup>, Yu Kudo<sup>1,\*2</sup>, Kazuhiko Kuribayashi<sup>2</sup>, Yuki Watanabe<sup>3</sup> and Takehiko Ishikawa<sup>4,5</sup>

<sup>1</sup>Department of Advanced Materials Science and Engineering, Chiba Institute of Technology, Narashino 275-0016, Japan

<sup>2</sup>Research Liaison Centre, Chiba Institute of Technology, Chiba Institute of Technology, Narashino 275-0016, Japan

<sup>3</sup>A.E.S. Co. Ltd., Tsukuba 305-0032, Japan

<sup>4</sup>Institute of Space and Astronautical Science, Japan Aerospace Exploration Agency, Tsukuba 305-8505, Japan

<sup>5</sup>SOKENDAI (The Graduate University for Advanced Studies), Sagami-hara 252-5210, Japan

Density of liquid titanium was measured free from any contamination over wide temperature range of 1640 and 2090 [K] including the undercooling condition by electrostatic levitator (ESL). When the diameter of upper electrode of ESL was modified to be smaller than that of lower one, it was decreased the uncertainty contribution of the droplet volume estimated from its image with respect to the density measurement by 30% through the suppression of the horizontal movement of the levitated droplet. The expanded uncertainties of the measurement plot were less than only  $\pm 1.4\%$  when the coverage factor  $k = 2$  was selected. Furthermore, it was evaluated the expanded uncertainty in the temperature dependence of density for liquid titanium expressed by a primary approximation of the plots.

[doi:10.2320/matertrans.L-M2017835]

(Received June 13, 2017; Accepted September 4, 2017; Published October 20, 2017)

**Keywords:** density, liquid titanium, electrostatic levitation, uncertainty in measurement

## 1. Introduction

Simulating a phase transition, such as crystallization and vitrification, requires highly accurate density, which is used as one of fundamental order parameters. However, using the conventional container method, it is difficult to measure accurate density of melt for high melting point materials such as titanium, because the sample is usually contaminated by the measurement device at elevated temperatures.

To avoid any contamination during the density measurement of liquid high melting point materials, container-free techniques such as electromagnetic levitation (EML) and electrostatic levitation (ESL) were employed<sup>1-5</sup>. These techniques achieve deep undercooling during measurement, due to absence of a container wall which acts as a heterogeneous nucleation site of solidification. However, the reported data of the density for liquid titanium still show discrepancies, particularly in the temperature coefficient, as shown in Fig. 1, even when container-free techniques are employed.

The density data of liquid titanium reported by Lee *et al.*<sup>1</sup> and Ishikawa and Paradis<sup>2</sup> using ESL show comparatively good agreement over wide temperature range including undercooling state. Saito *et al.*<sup>3</sup> also measured the similar temperature dependence of density for liquid titanium by using EML.

However, the density measured by Paradis and Rhim<sup>4</sup> using ESL is much higher than those of the above literature at low temperature, so the absolute value of temperature coefficient becomes twice as large. Although Zhou *et al.*<sup>5</sup> also reported such a large temperature coefficient by using EML, the reported density is much lower than that of other literature at high temperature.

For the discrepancies between the literature data on density of liquid titanium measured by container-free tech-

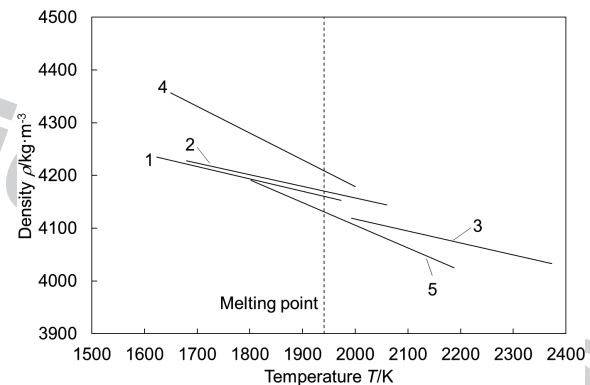


Fig. 1 Literature data reported for density for liquid titanium measured by container-free techniques. (1: Lee *et al.*<sup>1</sup>, 2: Ishikawa & Paradis<sup>2</sup>, 3: Saito *et al.*<sup>3</sup>, 4: Paradis & Rhim<sup>4</sup>, and 5: Zhou *et al.*<sup>5</sup>)

niques of EML and ESL, several possible reasons involving volume estimation and temperature measurement of sample are considered. Volume of a levitated droplet, necessary for the density calculation, is estimated from its side view monitored by a high-speed camera, under the assumption that the droplet shape is rotationally symmetrical with respect to the vertical axis. However, it is difficult to estimate an accurate droplet volume when the levitated droplet shows surface oscillations, because the above assumption is not always satisfied<sup>6</sup>. Comparatively large surface oscillations are usually induced in the electromagnetically levitated droplet, unless a strong static magnetic field is superimposed<sup>7,8</sup>.

A blurred image of the droplet, which is often caused from its high-temperature luminescence, could lead to an incorrect estimation of the volume. Translational oscillation of the droplet would also induce an incorrect estimation of the volume: if the droplet moves to back and forward from the reference position at which the camera is set for monitoring, the volume of the droplet is under- and overestimated. In the EML technique, a levitated droplet usually shows translational oscillation, due to an inhomogeneous distribution in

\*<sup>1</sup>Corresponding author, E-mail: shumpei.ozawa@it-chiba.ac.jp

\*<sup>2</sup>Graduate Student, Chiba Institute of Technology. Present address: Heraeus Electro-Nite, Ichikawa 272-0015, Japan

the magnetic field of the levitation coil<sup>7-9</sup>). In the ESL technique, it is difficult to suppress the translational oscillation of a droplet having low density and high vapor pressure such as titanium. A light sample is sensitively moved by a small change of electrostatic force. Evaporation of the sample not only decreases the sample mass, but also varies quantity of electric charge of the droplet, which is necessary for electrostatic levitation.

Since the center of the sample gets out from the line of sight of a pyrometer, translational oscillation of a droplet would also cause a noise and error in the temperature measurement. For a very small sample usually used in ESL, the suppression of the translational oscillation of the droplet is particularly important.

Recently, Okada *et al.*<sup>10</sup>) reported that the translational oscillation of the electrostatically levitated sample can be suppressed when the diameter of the upper electrode of the ESL was modified to be smaller than that of the lower one; the distribution of a conical electrical field induced from the modified electrodes improved horizontal position stability of the levitated sample.

In this study, density of liquid titanium was measured over a wide temperature range, including undercooling state, by ESL equipped with the modified electrodes in which the upper electrode has a smaller diameter than that of the lower electrode. To permit an accurate determination of the droplet contour, a backlight system was employed for its observation. Furthermore, high purity titanium was used as a sample. The purpose of this study was to accurately measure density of liquid titanium, to settle the discrepancy in the literature data.

## 2. Experiment Procedure

Figure 2 exhibits a schematic diagram of ESL apparatus of the Japan Aerospace Exploration Agency (JAXA) used in this study. The basic design of the ESL is similar to that developed by Rhim *et al.*<sup>11</sup>) Details of the facility are described elsewhere<sup>12</sup>). The chemical composition of high purity titanium used in this study is exhibited in Table 1. A piece of cubic sample of about 22 [mg] was placed between a pair of

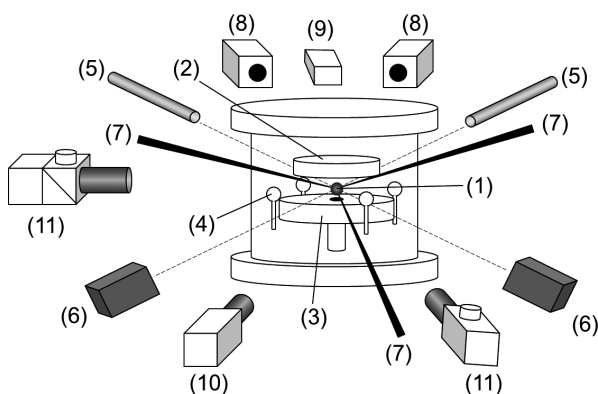


Fig. 2 Schematic view of the electrostatic levitation furnace and its diagnostic apparatus: (1) sample, (2) upper electrode, (3) lower electrode, (4) side electrodes, (5) He-Ne lasers, (6) position detectors, (7) CO<sub>2</sub> laser beams, (8) pyrometers, (9) mercury lamp, (10) CCD camera, (11) CCD cameras with telephoto objective lens.

parallel disk electrodes installed in a vacuum chamber. After the chamber was evacuated to the order of 10<sup>-5</sup> [Pa], the positively charged sample was electrostatically levitated by applying a high voltage between the electrodes. To improve horizontal stability of the levitated sample, the upper electrode was modified to have a smaller diameter ( $\phi$ 10 mm) than that of the lower one ( $\phi$ 25 mm), at which distribution of a conical electrical field induces a restoring force to move the sample toward the center of the electrodes, as numerically shown in Fig. 3<sup>13</sup>). Although the surfaces of iso-electric potential are almost flat between the conventional ESL electrodes with the same diameter (Fig. 3 (a)), it shows gradient<sup>13</sup>) when the diameter of the upper electrode becomes small (Fig. 3 (b)).

The levitated sample was melted and then heated by irradiations of 100 W CO<sub>2</sub> laser from three directions, with 120 degrees difference in the horizontal plane, to minimize horizontal movement of the levitated sample and enhance the temperature homogeneity<sup>14</sup>).

The sample temperature was monitored by using single-color pyrometer, at which the emissivity was adjusted to make the plateau temperature of the liquid phase after the recalescence indicate the equilibrium melting point of titanium. Although the period of the plateau temperature was only about 0.1 sec, sampling rate of the pyrometer used in this study (120 Hz) was sufficiently high to detect it.

The sample image was continuously observed from the horizontal direction by three high-speed CCD cameras, in conjunction with temperature while cooling the sample after turning off the laser irradiation. To determine the accurate sample contour, a background light of mercury lamp was employed, together with high-pass filter inserted in front of

Table 1 Chemical composition of titanium sample (mass ppm).

Ti	Ag	Al	B	Bi	Ca	Cd
Bal.	<0.02	0.69	<0.01	<0.01	<1	<0.05
Co	Cr	Cu	Fe	K	Mg	Mn
<0.01	0.39	0.4	0.35	<0.01	<0.01	0.1
Mo	Ni	P	Si	Sn	Th	U
<0.05	0.54	<0.01	1.4	<0.05	<0.0001	<0.0001
V	W	Zn	C	N	O	S
0.03	<0.01	<0.05	<10	<10	110	<10

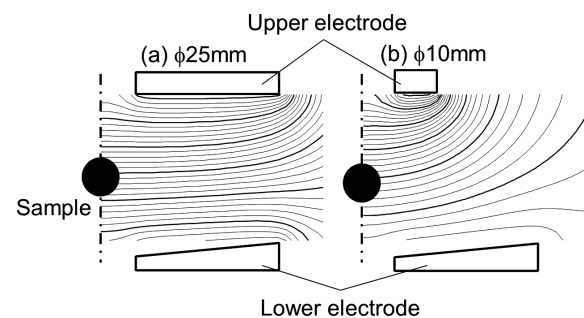


Fig. 3 Distribution difference of electric field between the electrodes by a numerical analysis, when the diameter of upper electrode is decreased from (a) 25 mm to (b) 10 mm.

the cameras<sup>15</sup>). Luminosity (mainly in the infrared) of a high temperature sample usually blinds its optical image.

The contour of the droplet image was numerically fitted by the following series of Legendre polynomials  $P_n(\cos\theta)$  of order five,

$$R(\theta) = \sum_{n=0}^5 c_n P_n(\cos\theta) \quad (1)$$

where  $R(\theta)$  is length from the center of gravity to the edge for the droplet,  $\theta$  is the polar angle, and  $c_n$  is the coefficients. Furthermore, the dimension of observed image was calibrated by levitating a solid reference sphere having a precisely known diameter under identical conditions.

Since the electrostatically levitated droplet was axi-symmetric, its volume  $V$  was calculated from each of the fitted data of side view, by using the following equation,

$$V = \frac{2\pi}{3} \int_0^\pi R(\theta)^3 \sin\theta d\theta \quad (2)$$

The mass of liquid sample corresponding to its temperature during cooling was calculated from the measured value after solidification, in consideration of the following evaporation rate measured by using the same ESL<sup>16</sup>.

$$e(T)(\text{mg/s}) = 5.13 \times 10^{-13} \exp(1.17 \times 10^{-2}T) \quad (3)$$

The density of liquid titanium for each temperature was determined from the sample mass  $M$  divided by the volume  $V$ .

$$\rho = \frac{M[\text{kg}]}{V[\text{m}^3]} \quad (4)$$

Uncertainty in the density measurement was evaluated based on GUM (ISO Guide to the Expression of Uncertainty in Measurement)<sup>17</sup>.

### 3. Results

Since the electrostatic levitation technique is based on Coulomb forces acting on charged sample placed within an electrostatic field, the experimental chamber was evacuated to the order of  $10^{-5}$  [Pa] to suppress discharges from electrodes in this study. Although titanium oxides are formed under the vacuum condition of  $10^{-5}$  [Pa] below 2100 K from a simple thermodynamic calculation using the Gibbs energy of oxides formations, no appreciable oxide was detected in the liquid sample. If some oxides is formed during the experiment, it can be detected in both the droplet image and the temperature profile because it has a higher emissivity. Very high oxygen solubility of liquid titanium may prevent the sample oxidation.

Figure 4 shows a typical cooling curve for the titanium sample levitated by the ESL. When the irradiations of all the heating lasers were shut off after the sample was sufficiently heated above the melting point, the sample temperature was deeply undercooled due to absence of container wall which acts as a heterogeneous nucleation site for solidification, and then increased sharply due to a recalescence. The recalescence was also confirmed from the time sequence of the corresponding droplet images. From these results, it was con-

firmed that the sample was in liquid state at segment a-b of Fig. 4. Furthermore, careful inspection of the temperature profile revealed very short period of plateau temperature which corresponds to the melting point of titanium sample after the recalescence.

Figure 5 shows the variation of the horizontal sample position during radiative cooling corresponding to segment a-b of Fig. 4 after shutting off the laser heating. Although the irradiation of heating laser from three directions can minimize the horizontal movement of levitated sample due to photon momentum transfer and local evaporation of the sample<sup>14</sup>), it also introduces an unbalanced force, enough to change the stable levitation position of the sample at the horizontal direction. As a result, horizontal displacement of the levitated sample is usually induced instantaneously just after shutting off the irradiation, followed by a translational oscillation of the sample. However, it is much suppressed by using the modified configuration of electrode ( $\odot$ ) having a smaller upper electrode, since the initial movement of the sample is reduced from about 200  $\mu\text{m}$  to 30  $\mu\text{m}$ .

Figure 6 exhibits the density of liquid titanium as a function of temperature, measured by ESL equipped with the modified configuration of electrode, together with the literature data for comparison<sup>1-5</sup>). The density of liquid titanium

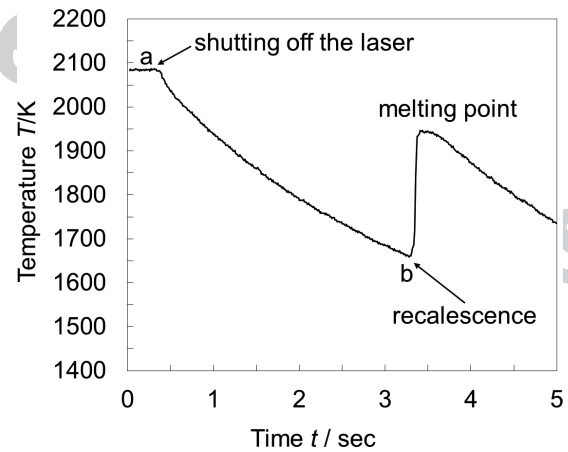


Fig. 4 Typical cooling curve of titanium sample levitated by the ESL after shutting off the irradiation of heating laser.

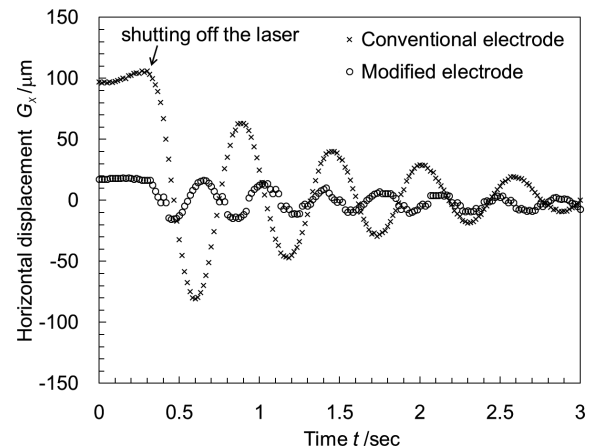


Fig. 5 Variation of the horizontal sample position during radiative cooling corresponding to the segment a-b of Fig. 4.

was measured over the wide temperature range of about 450 [K] between 1640 [K] and 2090 [K], including the undercooling region. Since the measured density exhibits a linear temperature dependence, it can be described by a primary approximation of the plots as follows.

$$\rho_{\text{Ti}}(T) = -0.23762(T - 1941) + 4193 \text{ [kg} \cdot \text{m}^{-3}], \quad (5)$$

where the intercept (4193 [kg · m<sup>-3</sup>]) corresponds to the density of liquid titanium at the melting point (1941 K). The absolute value of temperature coefficient of the density for liquid titanium measured in this study is about half of the literature data reported by Paradis & Rhim<sup>4</sup>) and Zhou *et al.*<sup>5</sup>) Whereas, the temperature dependence of density measured in this study agrees well with the literature data reported by Lee *et al.*<sup>1</sup>), Ishikawa and Paradis<sup>2</sup>), and Saito *et al.*<sup>3</sup>) The differences of the absolute values of the density and its temperature coefficient are only within about 1.4% (60 kg · m<sup>-3</sup>) and 4.3% (0.01 kg · m<sup>-3</sup> · K) between these studies, respectively.

## 4. Discussion

### 4.1 Uncertainty for the measurement plot

In this section, to support the validity of our measurement

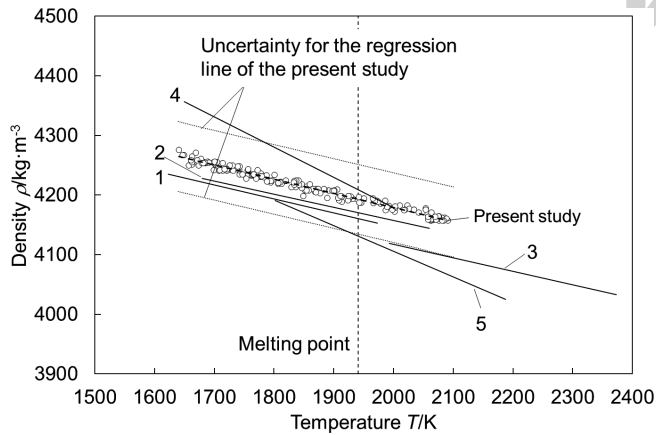


Fig. 6 Density of liquid titanium measured by ESL equipped with the modified configuration of electrodes, together with the literature data obtained by using container-free techniques. (1: Lee *et al.*<sup>1</sup>), 2: Ishikawa & Paradis<sup>2</sup>), 3: Saito *et al.*<sup>3</sup>), 4: Paradis & Rhim<sup>4</sup>), and 5: Zhou *et al.*<sup>5</sup>) The dotted lines correspond to uncertainty for the regression line calculated from measurement plots of this study.

result for density of liquid titanium, uncertainty for the measurement was evaluated based on GUM<sup>17</sup>). As mentioned in section 2, the mass of the levitated droplet used for density calculation  $M$  was estimated from the measured value after solidification, in consideration of its evaporation. The volume of droplet was determined from its 2-D image observed from the horizontal direction by high-speed video camera. The unit of droplet diameter was converted from pixels [px] into meters [m] by using the reference sphere, the diameter of which was measured by a micrometer. Therefore, the main sources of uncertainty in the measurement are from measured value of sample mass after experiment ( $m$ ), amount of sample evaporation ( $e$ ), numerical fitting of droplet contour ( $f$ ), diameter of droplet image in pixel units ( $d_p$ ), diameter of reference sphere in metric units ( $d_r$ ), and droplet volume converted from the 2D image ( $V$ ). The combined standard uncertainty in the density measurement  $u_c(\rho)$  can be evaluated from the uncertainty contributions  $u_\rho(i)$  of each source as follows,

$$u_c(\rho) = \sqrt{\begin{aligned} &(u_\rho(m))^2 + (u_\rho(e))^2 + (u_\rho(f))^2 \\ &+ (u_\rho(d_p))^2 + (u_\rho(d_r))^2 + (u_\rho(V))^2 \end{aligned}} \quad (6)$$

$u_\rho(i)$  is obtained from the products of the individual standard uncertainty  $u(i)$  and sensitivity coefficient  $c(i)$  for each source. Table 2 shows the uncertainty budget in the density measurement, when the largest value of the combined standard uncertainty was obtained within all plots, as the representative example. The standard uncertainty of the measured value of sample mass after experiment,  $u(m)$ , was calculated from the resolution of our electronic balance of  $0.01 \times 10^{-6}$  [kg].  $u(e)$  was evaluated from the change of the sample mass of  $0.01 \times 10^{-6}$  [kg] during measurement. Since the electrostatically levitated droplet shows as spherical,  $u(f)$  was obtained as the estimated standard deviation of pixels corresponding to the radius of droplet image when it was measured at 400 different points; the square of deviations of the detected radius was 150 [px<sup>2</sup>].  $u(d_p)$  was calculated as the detectable minimum length of droplet image, which is 1 [px].  $u(d_r)$  was evaluated from the measurement resolution of a micrometer.  $u(V)$  was calculated as the estimated standard deviation of the volume of the reference sphere, when it was estimated from the droplet image a few dozen times.

Sensitivity coefficient  $c(i)$  was evaluated by the partial derivative of each uncertainty source with respect to eq. (4) in

Table 2 Uncertainty budget of density measurement of liquid titanium by ESL equipped with the modified configuration of electrodes.

Source	Type	Value	Divisor	Standard uncertainty $u(i)$	Sensitivity coefficient $c(i)$	Uncertainty contribution $u_\rho(i)$
Measured value of sample mass after experiment, $m$	B	$0.5 \times 10^{-8}$ [kg]	$\sqrt{3}$	$2.8868 \times 10^{-9}$ [kg]	$1.9605 \times 10^8$ [m <sup>-3</sup> ]	$0.56595$ [kg · m <sup>-3</sup> ]
Amount of sample evaporation, $e$	B	$0.5 \times 10^{-8}$ [kg]	$\sqrt{3}$	$2.8868 \times 10^{-9}$ [kg]	$1.9605 \times 10^8$ [m <sup>-3</sup> ]	$0.56595$ [kg · m <sup>-3</sup> ]
Numerical fitting of droplet contour, $f$	A	0.61314 [px]	1	0.61314 [px]	$-42.598$ [kg · m <sup>-3</sup> · px <sup>-1</sup> ]	$-26.119$ [kg · m <sup>-3</sup> ]
Diameter of droplet image, $d_p$	B	0.5 [px]	$\sqrt{3}$	0.28868 [px]	$-42.598$ [kg · m <sup>-3</sup> · px <sup>-1</sup> ]	$-12.297$ [kg · m <sup>-3</sup> ]
Diameter of reference sphere, $d_r$	B	$0.5 \times 10^{-6}$ [m]	$\sqrt{3}$	$2.8868 \times 10^{-7}$ [m]	$-6.2147 \times 10^6$ [kg · m <sup>-4</sup> ]	$-1.7940$ [kg · m <sup>-3</sup> ]
Volume converted from droplet image, $V$	A	$4.2399 \times 10^{-12}$ [m <sup>3</sup> ]	1	$4.2399 \times 10^{-12}$ [m <sup>3</sup> ]	$-8.3829 \times 10^{11}$ [kg · m <sup>-6</sup> ]	$-3.5543$ [kg · m <sup>-3</sup> ]

Combined uncertainty,  $u_c(\rho)$ : 29.153 [kg · m<sup>-3</sup>]

Expanded uncertainty,  $U$ : 58.31 [kg · m<sup>-3</sup>] (coverage factor  $k_p = 2$  is selected.)

consideration of the following volume formula of the sphere,

$$V = \frac{\pi}{6}(a \cdot d_p)^3 \quad (7)$$

where  $a$  is the coefficient for converting  $d_p$  into metric units.

$$c(m) = c(e) = \frac{\partial \rho}{\partial M} = \frac{1}{V} \quad (8)$$

$$c(f) = c(d_p) = \frac{\partial \rho}{\partial d_p} = \frac{-18M}{\pi \cdot a^3 \cdot d_p^4} \quad (9)$$

$$c(d_r) = \frac{\partial \rho}{\partial d_r} = \frac{-18M}{\pi \cdot d_r^4} \quad (10)$$

$$c(V) = \frac{\partial \rho}{\partial V} = \frac{-M}{V^2} \quad (11)$$

When coverage factor  $k_p = 2$  is selected to expand the uncertainty in our measurement plots to satisfy 95.45% confidence, the maximum value of it was calculated as  $\pm 58.31$  [ $\text{kg} \cdot \text{m}^{-3}$ ], corresponding to about  $\pm 1.37\%$  for the measurement plots. This indicates that the uncertainty of our density measurement is at a sufficiently low level. The measured density of this study agrees very well with the literature data of Lee *et al.*<sup>1)</sup>, Ishikawa and Paradis<sup>2)</sup>, and Saito *et al.*<sup>3)</sup> within the uncertainty in the measurement.

Although the uncertainty contribution of the estimation of droplet volume,  $u_\rho(V)$ , was decreased from  $-4.93$  [ $\text{kg} \cdot \text{m}^{-3}$ ] to  $-3.55$  [ $\text{kg} \cdot \text{m}^{-3}$ ] (became 70%) when the horizontal movement of the droplet was suppressed by using the modified configuration of electrodes in this study (see Fig. 5), the combined uncertainty  $u_c(\rho)$  was reduced by only 0.4 [ $\text{kg} \cdot \text{m}^{-3}$ ] (less than 0.7%) because  $u_\rho(V)$  is more than 7 times smaller than  $u_\rho(f)$ , and 3 times smaller than  $u_\rho(d_p)$  as shown in Table 2. This result indicated that it is crucial to improve resolution of the droplet image, to reduce uncertainty in density measurement by ESL.

#### 4.2 Uncertainty for the temperature dependence of measured density

To utilize the measurement result of density for liquid titanium effectively, the uncertainty should be described not only in the measurement plots, but also in temperature dependence. Although the absolute value of the temperature coefficient for the density of liquid titanium measured in this study agreed well with the literature data reported by Lee *et al.*<sup>1)</sup>, Ishikawa and Paradis<sup>2)</sup>, and Saito *et al.*<sup>3)</sup>, it is about a half of that reported by Zhou *et al.*<sup>4)</sup> and Paradis and Rhim<sup>5)</sup>. The uncertainty of eq. (5) is evaluated here. The linear approximate expression for the temperature dependence of density can be described as follows, by using the arithmetic mean values of the measured density  $\bar{\rho}$  and temperature  $\bar{T}$ ,

$$\rho_{\text{Ti}}(T) = \widehat{\beta}(T - \bar{T}) + \bar{\rho}, \quad (12)$$

where  $\widehat{\beta}$  is the temperature coefficient of density. The uncertainty of this regression line  $u_c(\rho_T)$ , provided on the assumption that the uncertainty of temperature is neglected, can be evaluated from the following equations,

$$(u_c(\rho_T))^2 = (T - \bar{T})^2 \cdot (u(\widehat{\beta}))^2 + (u(\bar{\rho}))^2 \quad (13)$$

$$(u(\widehat{\beta}))^2 = \frac{\widehat{\sigma}_e^2 + (u_c(\rho))^2}{\sum(T_i - \bar{T})^2} \quad (14)$$

$$(u(\bar{\rho}))^2 = \frac{\widehat{\sigma}_e^2}{n} + (u_c(\rho))^2 \quad (15)$$

$$\widehat{\sigma}_e^2 = \frac{\sum[\rho_i - \{\widehat{\beta}(T_i - \bar{T}) + \bar{\rho}\}]^2}{n - 2} \quad (16)$$

where  $\widehat{\sigma}_e^2$  is the residual variance of the measured density, and  $n$  is the number of measuring plots. From these equations, the expanded uncertainty of the temperature coefficient of density for liquid titanium measured in this study,  $U(\widehat{\beta})$ , was evaluated as  $\pm 3.027 \times 10^{-2}$  [ $\text{kg} \cdot \text{m}^{-3} \cdot \text{K}^{-1}$ ], when the coverage factor of  $k = 2$  was selected. Furthermore, that of the eq. (5) is expressed as follows,

$$(U(\rho_T))^2 = 1.0285 \times 10^{-3}(T - 1854)^2 + 3400.1 \quad (17)$$

These results confirmed that the temperature dependence of the density for liquid titanium measured in this study is identical with the literature data reported by Lee *et al.*<sup>1)</sup>, Ishikawa and Paradis<sup>2)</sup>, and Saito *et al.*<sup>3)</sup> within the uncertainty in the measurement. Even when the coverage factor of  $k_p = 3$  is selected to expand the uncertainty in our measurement to satisfy 99.73% confidence, the temperature coefficient of this study was quite different from that reported by Zhou *et al.*<sup>5)</sup> and Paradis and Rhim<sup>4)</sup>.

#### 5. Summary

To measure an accurate density of liquid titanium over a wide temperature range including undercooling condition by ESL, the horizontal movement of the levitated sample was greatly suppressed by using a modified configuration of electrodes, in which the diameter of upper electrode was smaller than that of lower electrode. Uncertainty in the measurement was evaluated based on GUM.

The temperature dependence of the density for liquid titanium was described by a primary approximation of the plots, as follows.

$$\rho_{\text{Ti}}(T) = -0.23762(T - 1941) + 4193 \text{ [kg} \cdot \text{m}^{-3}\text{]} \\ (1640 \text{ K} - 2090 \text{ K})$$

This result agreed well with the literature data reported by Ishikawa and Paradis<sup>2)</sup>, Lee *et al.*<sup>1)</sup>, and Saito *et al.*<sup>3)</sup>

The maximum value of the expanded uncertainty between the measurement plots was  $\pm 58.31$  [ $\text{kg} \cdot \text{m}^{-3}$ ] ( $\pm 1.37\%$ ) when coverage factor  $k_p = 2$  was selected. Suppression of horizontal movement of levitated droplet by using modified electrodes decreased the uncertainty contribution of the estimation of droplet volume by about 30% in the measurement. It was clarified that resolution of the droplet image should be improved to further decrease combined uncertainty of the density measurement by ESL, since the uncertainty contribution regarding the droplet image is much higher than other factors.

The expanded uncertainties for temperature dependence of the density for liquid titanium and its temperature coefficient were evaluated as follows, respectively,

$$U(\rho_T) = \sqrt{1.0285 \times 10^{-3}(T - 1854)^2 + 3400.1} \text{ [kg} \cdot \text{m}^{-3}\text{]}$$

$$U(\widehat{\beta}) = \pm 3.027 \times 10^{-2} \text{ [kg} \cdot \text{m}^{-3} \cdot \text{K}^{-1}\text{]}$$

### Acknowledgements

This work was partially supported by JSPS KAKENHI. Grant number 24760617. One of the authors (YK), acknowledges support of the Sasakawa Scientific Research Grant from The Japan Science Society.

### REFERENCES

- 1) G.W. Lee, S. Jeon, C. Park and D.-H. Kang: *J. Chem. Thermodyn.* **63** (2013) 1–6.
- 2) T. Ishikawa and P.-F. Paradis: *J. Electron. Mater.* **34** (2005) 1526–32.
- 3) T. Saito, Y. Shiraishi and Y. Sakuma: *Trans. ISIJ* **9** (1969) 118–26.
- 4) P.-F. Paradis and W.-K. Rhim: *J. Chem. Thermodyn.* **32** (2000) 123–33.
- 5) K. Zhou, H.P. Wang, J. Chang and B. Wei: *Chem. Phys. Lett.* **639** (2015) 105–08.
- 6) M. Adachi, T. Aoyagi, A. Mizuno, M. Watanabe, H. Kobatake and H. Fukuyama: *Int. J. Thermophys.* **29** (2008) 2006–2014.
- 7) S. Ozawa, T. Koda, M. Adachi, K. Morohoshi, M. Watanabe and T. Hibiya: *J. Appl. Phys.* **106** (2009) 034907.
- 8) H. Yasuda, I. Ohnaka, Y. Ninomiya, R. Ishii, S. Fujita and K. Kishio: *J. Crys. Growth* **260** (2004) 475–485.
- 9) N. Takenaga, S. Ozawa, T. Hibiya, H. Kobatake, H. Fukuyama, S. Awaji and M. Watanabe: Proceedings of 57th International Astronautical Congress, Valencia, Spain, 2–6 October 2006, (International Astronautical Federation) pp. 627–632.
- 10) J.T. Okada, T. Ishikawa, Y. Watanabe and P.-F. Paradis: *J. Chem. Thermodyn.* **42** (2010) 856–859.
- 11) W.K. Rhim, S.K. Chung, D. Barber, K.F. Man, G. Gutt, A.A. Rulison and R.E. Spjut: *Rev. Sci. Instrum.* **64** (1993) 2961–2970.
- 12) T. Ishikawa, P.-F. Paradis, T. Itami and S. Yoda: *Meas. Sci. Technol.* **16** (2005) 443–451.
- 13) P.-F. Paradis, T. Ishikawa, R. Fujii, S. Yoda: *Heat Transfer - Asian Research* **35** (2006) 152–164.
- 14) P.-F. Paradis, T. Ishikawa and S. Yoda: *Space Technol.* **22** (2002) 81–92.
- 15) T. Ishikawa, P.-F. Paradis and S. Yoda: *Rev. Sci. Instrum.* **72** (2001) 2490–2495.
- 16) P.-F. Paradis, T. Ishikawa and S. Yoda: *European J. Phys. Appl. Phys.* **22** (2003) 97–101.
- 17) Guide to the Expression of Uncertainty in Measurement (ISO, 1995).